Tilted Fiber Bragg Grating Biosensor with Peak-Tracking for Troponin-T Based Heart Disease Detection

Prathap P B[1], Raghuram K A[2], Sushma N[3], Deepika K C[4], Santhosh Kumar K B[5]
[1,2,3,4,5]*Member, Malnad College of Engineering, Hassan.*

***Abstract*—The prevalence of cardiovascular diseases has been increasing, particularly among individuals aged 35–45 years. Disorders such as Coronary Artery Disease (CAD) and Cerebrovascular Disease (CVD) often result in myocardial injury due to inadequate oxygen supply, leading to heart attacks. Cardiac Troponin-T (cTnT) serves as a specific and reliable biomarker for detecting cardiac muscle damage, as it is released into the bloodstream only after myocardial cell injury. This paper proposes a highly sensitive gold-coated Tilted Fiber Bragg Grating (TFBG) biosensor with an optimized tilt angle of 11° for efficient detection of cTnT. A single-stranded DNA aptamer immobilized on a 0.02 mm gold layer via gold–thiol bonding exhibits strong and selective binding affinity toward cTnT within the concentration range of 0.05–5 ng/mL. The aptamer–protein interaction modifies the refractive index of the coating, resulting in a wavelength shift in the TFBG spectrum. RCC-correlation using the Mexican-Hat wavelet enhances peak tracking accuracy near the Bragg wavelength. Simulation results demonstrate that the proposed sensor achieves high sensitivity and stability, enabling precise and early diagnosis of cardiac disorders.**

***Index Terms*—Aptamer Sequence, Fiber Bragg Grating, Biosensor, Gold Encapsulation, Peak Tracking, Refractive Index, Troponin-T.**

I. INTRODUCTION

Coronary artery disease (CAD) or coronary heart disease (CHD), cerebrovascular disease (CVD), peripheral artery disease (PAD), aortic atherosclerosis, and acute myocardial infarction (AMI) have long been major causes of death and are very dangerous to human life. Traditionally, electrocardiography (ECG) has been used to diagnose it, but ECG alone has not been enough. To overcome this constraint, the identification of cardiac biomarkers has been suggested as a more efficacious approach. Troponins, particularly cardiac troponin-T (cTnT), have demonstrated superior sensitivity and specificity in identifying myocardial injury among these biomarkers. Because this is one of the most dangerous diseases, we need diagnostic tests that are not only accurate but also quick, easy to get to, and cheap so that we can start therapy based on evidence as soon as possible. This review talks about new developments in biosensors and analytical tools that are specific to cTnT. It talks on the progress that has been made and the problems that still need to be solved in making easy-to-use, cheap, portable testing instruments that can quickly and accurately find these cardiac biomarkers on-site. The goal is to make it possible to diagnose and treat heart problems early on and effectively [1].

As health problems get worse, we need more accurate and reliable sensors to help us find and diagnose them early. This can not only lessen the number of deaths, but it can also stop more problems from happening by making sure that people get diagnosed and treated on time. To do some complicated medical tests, such finding cancer, blood tests, and protein analysis, you need reliable sensor technologies. Also, a lot of other uses, such biomechanical sensing, physiological monitoring, non-invasive procedures, and biosensing, need sensors that are very sensitive. Different analog sensors were made in the past to sense health. Optical sensors work better than typical electrical sensors because they are more sensitive, have better resolution, and are less affected by changes in the environment around them. Fiber Bragg Grating (FBG) sensors are very useful in healthcare settings for things like biomechanical sensing, physiological monitoring, non-invasive operations, and biosensing. TFBG is a promising technology for these uses because it has many unique benefits, such as being very sensitive, resistant to chemicals, flexible, and able to grow with the needs of the user [2].

Several studies in the past few years have looked at ways to improve Fiber Bragg Grating (FBG) designs so that they are more sensitive and resistant to changes in the local environment. These improvements can be made by changing the design, materials, and structure. On the other hand, temperature, stress, and viscosity can all change the refractive index of an FBG biosensor. This means that biosensors must be designed to stay very sensitive and accurate even when these things happen [2, 3]. Although attempts have been made to create different grating structures, like long-period gratings (LPG), phased grating FBG, super-structured FBG, and chirped FBG (CFBG), their performance is typically not as good as that of enhanced plasmonic FBG biosensors [5]. This restriction is mostly due to their reduced sensitivity to heat fluctuations. As stated previously, plasmonic biosensors are very sensitive to changes in the region of interest (ROI) because of changes in fluid viscosity and strain. This can affect how accurately they can follow peaks [1–4]. Recently, some have suggested using Tilted FBG (TFBG) designs with grating encapsulation for biosensing [6, 7]. But these designs still need to be improved so that they can handle unclear peaks and provide accurate resolution tracking [5, 8]. When it comes to real-world biosensing, TFBG is quite sensitive to changes in the surrounding refractive index, especially when this index is close to that of the cladding. In real-world situations, the attenuation bands move toward shorter wavelengths when the refractive index of the surrounding medium gets close to the cladding index. This is especially true when the surrounding refractive index suddenly rises.

In these situations, the coupling wavelength must change, especially when the refractive index of the surrounding area (or neighbor) is higher than the cladding index. For example, in biosensing jobs like finding cancer or analyzing proteins, the attenuation bands may move to shorter wavelengths as the refractive index of the surrounding material goes up from the ambient value (1, which is the air index) to a higher value that is closer to the cladding index. This shows that the TFBG sensor is quite sensitive to changes in the refractive index around it, especially as it gets close to the cladding index. This sensitivity can cause the coupling wavelength to change when the index next to it is higher than the cladding index. To improve the sensor's performance, the grating can be covered with a substance that interacts with the analyte outside the sensor. This changes the refractive index and shifts the transmission spectrum. This method can be used successfully for a number of biosensing activities [2–8].

This study presents the design and simulation of a highly sensitive gold-encapsulated Tilted Fiber Bragg Grating biosensor for the detection of Troponin-T levels, based on the aforementioned inferences and related domains. A certain aptamer sequence is stuck to the surface of the gold, which has a strong attraction to Troponin-T in the range of 0.05 to 5ng/mL. An aptamer is a short, single-stranded nucleic acid (RNA or DNA) that has been chosen because it can bind to a target molecule with a lot of affinity and specificity. In this scenario, the aptamer is made to stick to Troponin-T. The aptamer is stuck to a gold surface, probably using thiol groups (-SH) that can make strong covalent connections with the gold surface (via gold-thiol chemistry). Gold is a common material for biosensors because it is biocompatible and provides a stable surface for holding molecules in place. This lets the target molecules get trapped, which raises the refractive index of the coating material and causes a shift in the wavelength spectra. This is useful for biosensing jobs. Because the coating material has a greater refractive index than the cladding index, the spectral shift and coupling wavelength shifts help with biosensing duties. Simulations verified the wavelength spectrum shift indicative of biosensing functions.

The other sections of this paper are given as follows. Section II discusses the related work, which is followed by the proposed model in Section III. Section IV presents the proposed model, while the simulation results and allied research conclusions are discussed in Section V and Section VI, respectively.

II. LITERATURE SURVEY

Several studies have focused on the design and optimization of Fiber Bragg Grating (FBG) and Tilted Fiber Bragg Grating (TFBG)-based biosensors for biochemical and biomedical applications.

In [2], P. B. Prathap et al. presented a self-compensating gold-encapsulated TFBG structure for

peak-tracking biosensing. A 9°-tilted TFBG was simulated, and cross-correlation-based matched filtering was used to find the Bragg wavelength peaks for clinical analysis. We employed correlation vectors with greater peak intensities to accurately follow peaks, using the Mexican-Hat wavelet as a reference. The proposed sensor had a sensitivity of 0.9 nm/RIU and did a good job of reducing noise caused by strain, viscosity, and temperature. This made it good for biosensing both in vivo and ex vivo. In [3], the same scientists put forward a multilayer gold-encapsulated TFBG biosensor with a 10° tilt angle. A graphene oxide (GO) layer boosted plasmonic coupling and made it easier for antibodies to attach to antigens. The change in refractive index caused measurable changes in wavelength, which showed that it might be used for protein and immune detection.L. Han et al. [4] experimentally validated a Surface Plasmon Resonance (SPR)-based reflective fiber biosensor for the label-free detection of urine AQP2. A 50 nm gold-coated TFBG facilitated high-resolution refractive index detection with a threshold of 1.5 ng/mL, differentiating between healthy and nephropathic samples.

T. Guo et al. [5] presented a comprehensive review of TFBG principles, fabrication, and applications, including vibroscopes, accelerometers, micro-displacement sensors, and plasmonic biochemical sensors for detecting proteins and glucose. Sun et al. [9] developed a reflective micro-FBG biosensor for DNA hybridization using multilayer films of PEI, PAA, and ssDNA. This design improved thermal stability and detection sensitivity.

Korganbayev et al. [10] explored TFBG sensors for ex vivo laser ablation monitoring of hepatic tissue, demonstrating their dual capability in refractive index and temperature sensing. Lobry et al. [11] designed a plasmonic FBG demodulator using envelope intersection for detecting HER2 protein, aiding breast cancer diagnosis. Negahdary et al. [12] developed an electrochemical aptasensor for Troponin-T detection in the 0.05–5 ng/mL range, achieving 0.01 ng/mL detection limit with 95% sensitivity and specificity.

III. SYSTEM DESIGN

This part talks about the proposed biosensor model's architecture and how it will be built, with a focus on how it will be more reliable and sensitive. The suggested design is different from traditional biosensor setups, which use simple TFBG structures with simple encapsulations for plasmonic absorption. Instead, it focuses on improving both the grating structure and the coating layers to get better detection accuracy and sensitivity. The Tilted Fiber Bragg Grating (TFBG) structure is chosen as the main sensor element since it has been shown to be able to detect spectra with high resolution. The biosensor uses an 11° angled grating to increase spectrum reflection and make it easier to monitor peaks accurately. A 15 mm-long gold covering with a thickness of 0.02 mm is put over the grating area to improve plasmonic coupling and the effectiveness of molecule binding. Gold encapsulation increases reflectivity and enables effective biomolecular interactions. This leads to changes in surface density, viscosity, and refractive index in the cladding mode, which are all important for measuring wavelength shifts in biosensing.

A multi-layer coating method is used, with each layer making the coating more sensitive and particular. Additionally, a Troponin-T-specific aptamer is fixed to the gold surface via gold-thiol chemistry. The aptamer, which is a small single-stranded DNA molecule, has a strong binding affinity for Troponin-T in the range of 0.05–5 ng/mL. When the target binds, the local refractive index goes up, which causes a detectable shift in the spectral wavelength that acts as the biosensing signal? Fig. 1 shows the overall design of the proposed multi-layer coating-assisted TFBG biosensor. It shows how the structure and function work together to improve the detection of Troponin-T biomarkers in clinical settings.

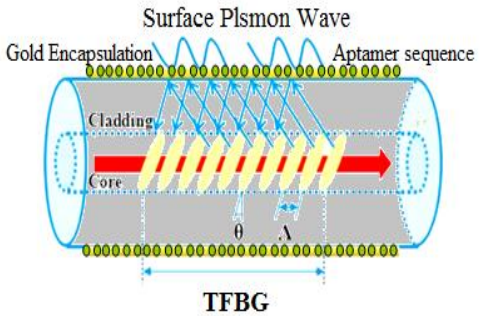

Fig. 1 Proposed TFBG biosensor design [3].

Figure 1 shows a diagram of the suggested TFBG biosensor. The tilt grating is shown at an angle of 11° and has a length of 15 mm. This study used MATLAB simulations, and making the design is not

possible right now, but this section gives the design parameters and functional details. The idea can be made practical and used in the actual world with hydrogen-loaded single-mode fibers, such the Corning SMF-28 type. The core diameter in the simulation model is 9 μm, and the cladding diameter stays at 120 μm. The scanning phase-mask technique can be used to make this design. A laser beam goes through a phase or amplitude mask in this method, which works as a diffractive optical element. The mask divides the entering beam into two diffraction orders, usually +1 and -1, with the same amount of power in each.

As stated before, to improve reflectivity 0.02 mm gold coating is done on the cladding surface, which can be done by using the ion-beam sputtering process. This way, only a small amount of the transmitted light actually goes through the grating. This light is then coupled into the cladding, which creates a lot of cladding modes. Now, in conjunction with the phase-matching criterion, for the proposed biosensor we determine the resonant wavelength for the i-th cladding mode by applying (1).

$$\lambda^{i}_{coupling} = \left(\eta^{i}_{eff-CLAD} + \eta_{eff.CORE}\right) \Lambda / \cos\theta \qquad (1)$$

In (1), $\eta_{eff.CORE}$ is the effective refractive index of the core mode, while the effective refractive index for the $i-th$ cladding mode is given by $\eta^{i}_{eff-CLAD}$. The other two parameters, Λ and θ, are the grating period and the tilt angle, respectively. Now, together with the design construct and the need that the surface plasmon wave on the top surface film be activated, the cladding model that meets the phase-matching criterion and dispersion is connected to the surface plasmon wave. In this situation, surface plasmon resonance would occur, particularly at the interface of the gold layer or medium. The energy of the cladding mode is then transferred to the surface plasmon waves, which lowers the energy of the cladding mode in the transmission spectrum. In the end, it makes a concave area [13]. This means that surface plasmon waves are typically still sensitive to the refractive index of nearby materials and any changes to it. There used to be a spectrum shift when the effective refractive index changed, which changed the wavelength and strength of the surface plasmon resonance. In the end, it affects the value of λ_coupling. In this context, the surrounding refractive index can be approximated by observing the variation in the peaks of the surface plasmon wavelength and its intensity [14] [15].

In our case, due to the plasmonic absorption$\eta_3 > \eta_{CLAD}$, the cladding mode doesn't undergo any internal reflection and hence behaves as a leaky mode FBG. The fiber then acts as a circular dielectric waveguide. Let, a_2 be the radius of the cladding mode, and η_d be the index about the cladding index, and η_3 or η_s be the surrounding index or coating material (post absorption) index. Then, in this case, the parameters β_{CLAD}, u_2, w_2, and v possess complex values and hence the Bessel functions might have complex arguments. On the other hand, if the propagation constant β_{CLAD} turns out to be complex, then it becomes significant to consider leaky modes. Now, in a single-mode fiber, the proposed TFBG can couple the fundamental core mode to the co-propagating cladding mode at the coupling wavelength given by (2).

$$\lambda_i^{(n)} = \left(\eta_{core}(\lambda_i) - \eta_{CLAD}{}^{(n)}(\lambda_i)\right)\Lambda \qquad (2)$$

In (2), $\lambda_i^{(n)}$ is the nth coupling wavelength, while $\eta_{core}(\lambda_i)$ indicates the effective refractive index of the core. $\eta_{CLAD}{}^{(n)}(\lambda_i)$ is the effective refractive index of the n-th cladding model, while Λ states the grating period. It indicates that whenever η_3 changes due to the absorption of the target molecule in coating, the propagation constant of cladding modes $\beta_{CLAD}^{(n)}$ and the refractive index of cladding model $\eta_{CLAD}{}^{(n)}(\lambda_i)$ changes that consequently would cause coupling wavelength $\lambda_i^{(n)}$ shift. We measured this wavelength shift to assess the biosensing task.

To sense accurately, it needs to be able to self-compensate, which could lower the peaks that don't matter. In this study, the Bragg-wavelength shift of the reflected TFBG signal was aligned with a used reference spectrum. In this study, the Mexican-Hat wavelet function was utilized to generate the reference spectra, with the Gaussian spectra response being the signal of interest. We looked at the Gaussian spectra signal (3) because the reflected gold-coated TFBG signal looks like it.

$$R(\lambda) = e^{-4*\ln 2\left(\frac{\lambda-\lambda_B}{\Delta\lambda_B}\right)^2} \qquad (3)$$

In (3), λ_B and $\Delta\lambda_B$ signify the central wavelength and 3-dB bandwidth, correspondingly. We fixed the

Bragg wavelength in the range of 1561nm - 1564 nm and the central peak was fixed at 1562.5 nm. Equation (4) defines the reference signal generated by using the Maxican-Hat wavelet function. In (4), λ_{Bref} is the reference spectral signal's center wavelength.

$$\Psi(\lambda) = \left[1 - \left(\frac{(\lambda - \lambda_{\mathrm{Bref}})}{\Delta\lambda_{\mathrm{Bref}}}\right)^2\right] e^{\left(\frac{(\lambda-\lambda_{\mathrm{Bref}})}{\Delta\lambda_{\mathrm{Bref}}}\right)^2} \quad (4)$$

To detect the peak signal, the self-compensating model used matched filtering, which finds the unknown peak in the spectral domain. It becomes essential for biosensing, as molecular viscosity induces numerous reflections [2], making peak detection crucial. The matching filter here made it possible to follow the best peaks across gold-encapsulated TFBG biosensors. In this study, the measured spectral response and the reference signal were coupled through RCC to develop the matching filter. It presumes that the peaks of the TFBG spectral signal and the reference signal must align. We used the least square (LS) approach to find peak (7) from the first derivatives of the TFBG spectra response and reference signal (5). We employed coupled mode theory (5) to figure out the reference signal, where k and S are the AC and DC coupling coefficients.

$$R(\lambda) = \frac{\sinh^2\left(\sqrt{k^2 - s^2}L\right)}{\cosh^2\left(\sqrt{k^2 - s^2}L\right) - \frac{s^2}{k^2}} \quad (5)$$

In (5), The DC self-coupling coefficient is given as s (6).

$$S = \frac{2\pi}{\lambda} \quad (6)$$

$$F(\lambda_\tau, \alpha) = \int_{-\infty}^{\infty} [R'(\lambda) - \alpha\Psi'(\lambda + \lambda_\tau)]^2 d\lambda \quad (7)$$

In (7), λ_τ states the peak's position (a delay parameter), where α is the unknown peak value. We solved LS problem (7) by minimizing the derivative with respect to the delay (λ_τ) and magnitude (α) parameters and finally yields $C(\lambda_\tau)$ and$\alpha(\lambda_\tau)$, given in (8) and (9), respectively. Here, $\lambda' = \lambda - \lambda_{\mathrm{Bref}}$ is the wavelength range to be selected for both reference spectra as well as the measured optical response.

$$C(\lambda_\tau) = \int_{-\infty}^{\infty} R(\lambda)\Psi'''(\lambda' + \lambda_\tau)d\lambda \quad (8)$$

$$\alpha(\lambda_\tau) = \frac{\int_{-\infty}^{\infty} R(\lambda)\Psi''(\lambda' + \lambda_\tau)d\lambda}{\int_{-\infty}^{\infty} [\Psi'(\lambda)]^2 d\lambda} \quad (9)$$

In (8), $C(\lambda_\tau)$ yields RCC output, obtained in-between the reference signal R(λ) and the third derivative of the measured spectral outputΨ (λ). RCC output yields the position of the zero-crossing points, presenting the point where 1st derivative of (7) becomes zero. The zero-crossing point was determined in accordance with equation (10-12).

$$C(\lambda_\tau) = 0 \quad (10)$$

$$\int_{-\infty}^{\infty} R(\lambda)\Psi'''(\lambda' + \lambda_\tau)d\lambda = 0 \quad (11)$$

$$\int_{-\infty}^{\infty} e^{-4*\ln 2\left(\frac{\lambda-\lambda_B}{\Delta\lambda_B}\right)^2} . C^{-8} . (\lambda^5 - A_1\lambda^4 + A_2\lambda^3 + A_3\lambda^2 + A_4\lambda - A_5)e^{-\frac{1}{2}\left(\frac{\lambda-l}{\Delta\lambda B_{\mathrm{ref}}}\right)^2} d\lambda = 0 \quad (12)$$

In (12), $l = \lambda B_{\mathrm{ref}} - \lambda_\tau$. $A_1, A_2, A_3, A_4,$ And A_5 are the differentiation coefficient. The zero-crossing point is measured by integration performed on (12) to equate as zero and thus it yields a zero-crossing point as (13).

$$\lambda_\tau = \lambda_{\mathrm{ref}} \quad (13)$$

The target wavelength peak was measured as per (14).

$$\alpha(\lambda_\tau) = \frac{\int_{-\infty}^{\infty} e^{-4*\ln 2\left(\frac{\lambda-\lambda_B}{\Delta\lambda_B}\right)^2} . C^{-8} . (\lambda^4 - B_1\lambda^2 + B_2\lambda^2 + B_2}{\int_{-\infty}^{\infty} \left[(\lambda - \lambda_{\mathrm{Bref}})(\lambda^2 - C_1\lambda - C_2)e^{-\frac{1}{2}\left(\frac{\Delta}{}\right.} \right.} \quad (14)$$

Substituting (13) from (14), the value of $\alpha(\lambda_\tau)$ becomes maximum at the central peakλB_{ref}, signifying the exact peak wavelength. In the presence of varied noise or interference over viscous test media, There might be more than one zero-crossing location at$\lambda_{\tau 1}, \lambda_{\tau 2}$, and$\lambda_{\tau 3}$. But there needs to be a single, distinct peak wavelength when the intensity $\alpha(\lambda_\tau)$ response occurs which remains the highest. To suppress irrelevant peaks from the measured spectra we modified (8) and (9) as (15) and (16), correspondingly.

$$C(\lambda_{\tau i}) = \int_{-\infty}^{\infty} \sum_{i=1}^{k} R_i(\lambda_i)\Psi_i'''(\lambda_i' + \lambda_{\tau i})d\lambda \quad (15)$$

$$\alpha(\lambda_{\tau i}) = \sum_{i=1}^{k} \frac{R_i(\lambda_i)\Psi_i'''(\lambda_i'' + \lambda_{\tau i})d\lambda}{\int_{-\infty}^{\infty}[\Psi_i'(\lambda_i)]^2 d\lambda} \quad (16)$$

In (15-16), $R_i(\lambda_i) = e^{-K\left(\frac{\lambda_i - \lambda_{B_i}}{\Delta\lambda_{B_i}}\right)^2}$, while $\lambda_{B_1}, \lambda_{B_2}, \lambda_{B_3}, \ldots, \lambda_{B_K}$ be the different TFBG peaks

$$\Psi_i(\lambda_i) = \left[1 - \left(\frac{\lambda_i - \lambda B_{refi}}{\Delta\lambda B_{refi}}\right)^2\right] e^{-K\left(\frac{\lambda_i - \lambda_{B_i}}{\Delta\lambda_{B_i}}\right)^2} \quad (17)$$

With (15), the zero-crossing point was obtained by equating $C(\lambda_{\tau i})$ as zero. At the detected zero-crossing points $\alpha(\lambda_{\tau i})$ remains the highest value signifying the target peak.

We created a MATLAB model that uses the core and cladding modes we talked about before to measure and plot the wavelength shift as the refractive index around it rises. To put it another way, the model measures how much the wavelength shift and peak variations change when the refractive index of the cladding gets closer to that of the surrounding medium.

IV. RESULTS AND DISCUSSION

This study proposes a multi-layer coating-assisted Tilted Fiber Bragg Grating (TFBG) biosensor for the high-sensitivity detection of cardiac Troponin-T. The design's goal is to make clinical diagnostic applications more sensitive, accurate, and scalable. The TFBG structure has a grating length of 15 mm and a tilt angle of 11°, which improves reflectivity and spectral resolution. A 0.02 mm gold layer surrounds the cladding zone. This makes plasmonic interaction stronger and the surface more stable. A Troponin-T-specific aptamer is fixed to the gold surface to make it possible to selectively identify biomolecules. This layer absorbs plasmonic energy. This arrangement of gold and aptamer in layers makes it easier for molecules to stick to each other, increases reflectivity, and makes it easier to detect changes in wavelength. Simulations based on MATLAB were used to test performance.

we assumed that the target molecular absorption at the coating surface over a longer period such as one house can increase the surrounding refractive index (i.e., η_3 or η_s). Therefore, we simulated the spectral outputs for the different surrounding indices (η_3=1.50 and 1.55). The results obtained are given in Fig. 2.

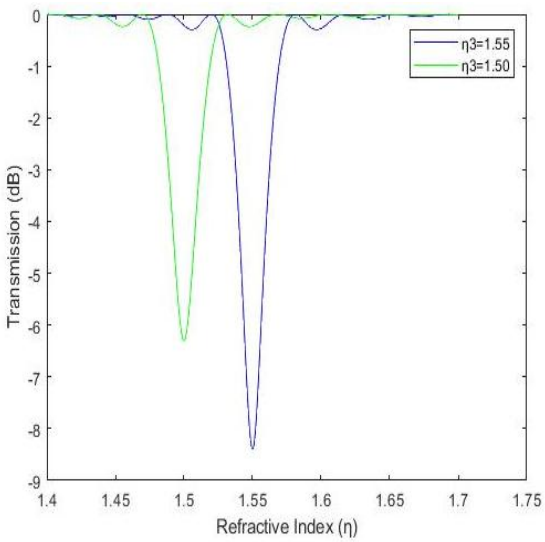

Fig.2 Transmission Spectrum for Different Refractive Indices

Figure 2 shows that changing the refractive index of the TFBG sensor's surface or surroundings causes a measurable change in both the wavelength and the amplitude. In accordance with the notion that plasmonic absorption at the coating surface leads to an increase in density and, consequently, the refractive index. We thought about using gold encapsulation as a metal layer with an aptamer sequence on top for plasmonic absorption. In real-world testing, the blood sample can be injected into the surface, which can then be soaked for a certain amount of time (in minutes, depending on how much solution is taken in). You can choose the sort of solution and its makeup here based on some clinical and calibration standards [7]. The outcome demonstrates that employing aptamer sequences as molecular absorbents can elevate the surrounding refractive index from 0.5 to 1. such, you can choose the soaking time or injection volume such that the change in effective refractive index and related amplitude (and coupling wavelength spectrum change) can be seen clearly. In short, the proposed design may produce a big enough spectrum shift and amplitude (in dB) changes with the right concentration and coating area. These changes could be used for biosensing tasks.

The simulation findings (Fig. 3(a)-Fig. 3(c)) show that changes in the refractive index unit (RIU) are linked to changes in the reflected optical spectra, with a shift rate of 0.30 nm per RIU. The

wavelength of the peak in the reference spectra was found to be 1562.2 nm. The simulation findings indicate that the reference peak spectra (Fig. 3(a)) encompass both peaks at 1562.6 nm and 1562.9 nm, which reside within the identical Bragg wavelength range. The reflected signal has its strongest peak at a wavelength of 1563.2 nm. In this case, the observed target spectra reveal a drop in intensity, even though the Bragg wavelength only changes a little.

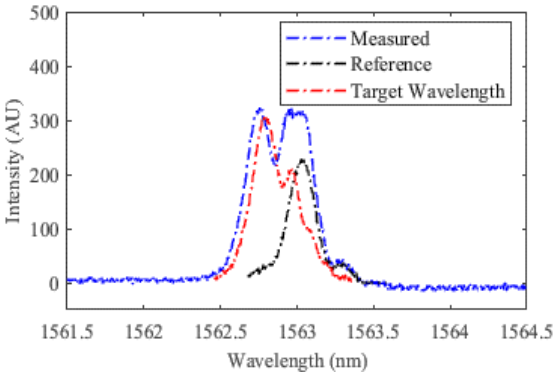

Fig.3 (a) Performance of peak tracking across various Bragg shifts

Fig.3(b) shows three distinct peaks, with wavelengths of 1562.6 nm, 1562.92 nm, and 1563.3 nm. The uncertainty in the Mexican Hat reference spectra could potentially lead to inaccurate clinical decisions by presenting false peaks.

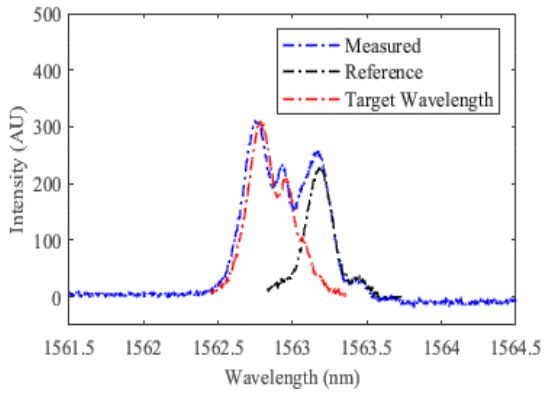

Fig.3(b) Peak tracking performance across various Bragg shifts, along with the corresponding measured and reference spectral responses.

The results in Fig.3(c) illustrate how the proposed self-compensation and matching filtering, supported by RCC-correlation, facilitate precise and accurate peak identification for biosensing.

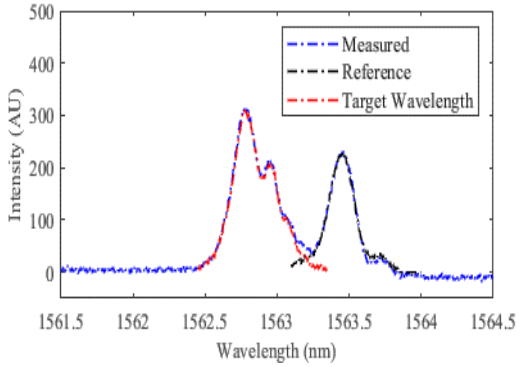

Fig.3 (c) Peak Tracking for Biosensing

By analyzing the simulation results (Fig. 4 and Fig. 5), it is evident that the increased reflectivity leads to a noticeable (or sufficiently large) shift in the Bragg wavelength (highlighted in yellow in Fig. 5), which is crucial for making accurate biosensing decisions. Additionally, the simulation results (Fig. 5) demonstrate that the proposed cross-correlation-driven matched filtering approach enhances the efficiency of the TFBG model, effectively reducing noise and improving sensitivity for biosensing tasks.

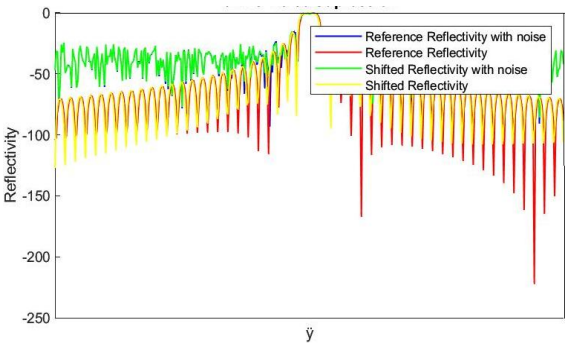

Fig.4 Bragg wavelength Shift without Peak Tracking

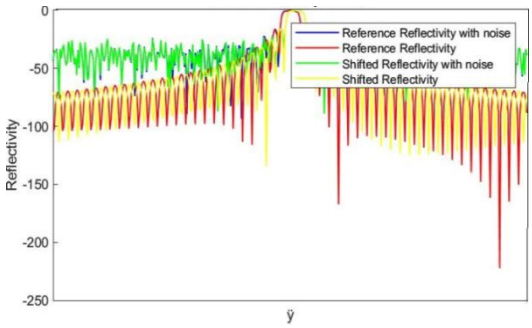

Fig. 5 Bragg wavelength shift with Peak Tracking

The results obtained clearly demonstrate that our proposed TFBG biosensor is effective for detecting Troponin-T to identify heart disease. The final conclusions and related inferences are provided in the following section.

V. CONCLUSION

In this research, we provide a highly sensitive biosensor utilizing a gold-coated Tilted Fiber Bragg Grating (TFBG) with an 11° tilt angle. A specific aptamer sequence is attached to the sensor's surface and held in place by a 0.02 mm thick layer of gold that was chosen because it is very biocompatible and chemically stable. This aptamer, which is a short single-stranded nucleic acid, has a strong affinity for Troponin-T at concentrations between 0.05 and 5 ng/mL. It attaches to the target molecule in a specific way using gold-thiol chemistry. When troponin-T binds to the coating, it causes a local rise in the coating's refractive index, which changes the sensor's wavelength spectrum in a way that can be seen. To boost detection accuracy, we applied RCC-correlation between reference and observed TFBG spectra. The Mexican-Hat wavelet was used as a reference to find zero-crossing points and correlation vectors that could be used to monitor the target spectral peak around the Bragg wavelength. This shift in the refractive index acts as a biosensing mechanism, and simulations show that this method works for finding Troponin-T. Performance characterization shows that the sensor has large wavelength shifts when biomolecules interact with it. This means it is very sensitive and might be used in many more biosensing applications.

REFERENCES

[1] Campu A, Muresan I, Craciun AM, Cainap S, Astilean S, Focsan M. Cardiac Troponin Biosensor Designs: Current Developments and Remaining Challenges. Int J Mol Sci. 2022 Jul 13;23(14):7728. doi: 10.3390/ijms23147728. PMID: 35887073; PMCID: PMC9318943.

[2] Prathap, P.B., Saara, K. Self-compensating gold-encapsulated tilted fiber Bragg grating for peak tracking based biosensing applications. J Opt 53, 2005–2019 (2024). https://doi.org/10.1007/s12596-023-01369-6.

[3] Prathap, P.B., Saara, K. Multilayer coating-assisted gold-encapsulated tilted fiber Bragg grating biosensor design. J Opt (2024). https://doi.org/10.1007/s12596-024-01711-6.

[4] L. Han et al., Specific Detection of Aquaporin-2 Using Plasmonic Tilted Fiber Grating Sensors. J. Lightwave Technol. 35(16), 3360–3365 (2017).

[5] T. Guo, F. Liu, B.-O. Guan, J. Albert, Tilted Fiber grating mechanical and biochemical sensors. Opt. Laser Technol. 78, 19–33 (2016).

[6] C. Massaroni, M. Zaltieri, D. Lo Presti, A. Nicolò, D. Tosi, E. Schena, Fiber Bragg grating sensors for cardiorespiratory monitoring: a review. IEEE Sens. J. 21(13), 14069–14080 (2021).

[7] C. Leitão et al., Cortisol in-fiber ultrasensitive plasmonic immuno-sensing. IEEE Sens. J. 21(3), 3028–3034 (2021).

[8] T. Guo, Á. González-Vila, M. Loyez, C. Caucheteur, Plasmonic optical fiber-grating immune-sensing: a review. Sensors 17(12), 2732 (2017).

[9] D. Sun, T. Guo and B. -O. Guan, "Label-Free Detection of DNA Hybridization Using a Reflective Microfiber Bragg Grating Biosensor with Self-Assembly Technique," in Journal of Lightwave Technology, vol. 35, no. 16, pp. 3354-3359, 15 Aug.15, 2017.

[10] S. Korganbayev, M. De Landro, A. Wolf, D. Tosi and P. Saccomandi, "Tilted Fiber Bragg Grating Measurements during Laser Ablation of Hepatic Tissues: Quasi-Distributed Temperature Reconstruction and Cladding Mode Resonances Analysis," in IEEE Sensors Journal, vol. 22(16), pp. 15999-16007, 2022.

[11] M. Lobry et al., "Plasmonic Fiber Grating Biosensors Demodulated Through Spectral Envelopes Intersection," in Journal of Lightwave Technology, vol. 39, no. 22, pp. 7288-7295, 15 Nov.15, 2021.

[12] Negahdary M, Behjati-Ardakani M, Heli H, Sattarahmady N. A Cardiac Troponin T Biosensor Based on Aptamer Self-assembling on Gold. Int J Mol Cell Med 2019; 8 (4) :271-282.

[13] J.-M. Renoirt, M. Debliquy, J. Albert, A. Ianoul, and C. Caucheteur, “Surface plasmon resonances in oriented silver nanowire coatings on optical fibers,” J. Phys. Chem. C, vol. 118, no. 20, pp. 11035–11042, May 2014.

[14] X. Qiu, X. Chen, F. Liu, B.-O. Guan, and T. Guo, “Plasmonic fiber-optic refractometers based on a high Q-factor amplitude interrogation,” IEEE Sensors J., vol. 16, no. 15, pp. 5974–5978, Aug. 2016.

[15] M. Z. Alam and J. Albert, “Selective excitation of radially and azimuthally polarized optical fiber cladding modes,” J. Lightw. Technol., vol. 31, no. 19, pp. 3167–3175, Oct. 1, 2013.